Indian Journal of Science and Technology, *Vol 11(2), DOI: 10.17485/ijst/2018/v11i2/120608, January 2018*
ISSN (Print) : 0974-6846
ISSN (Online) : 0974-5645

Numerical Simulation of Methane-Hydrogen Combustion in the Air: Influence on Combustion Parameters

Mohammed El Hadi Attia[1], Abderrahmane Khechekhouche[2] and Zied Driss[3]

[1]Department of Physics, Faculty of Science, University of El Oued, 39000 El Oued, Algeria; attiameh@gmail.com
[2]Renewable Energy development unit in Arid Zones (UDERZA), University of El-Oued, Algeria; Abder03@hotmail.com
[3]Laboratory of Electro-Mechanic Systems (LASEM), ENIS, University of Sfax, Tunisia; zied.driss@enis.tn

Abstract

Objectives: To study the behavior of these parameters following the variation of CH4-H2 fuels in air. **Methods/Statistical Analysis:** We simulated the behavior of the turbulent methane-hydrogen/air flame, generated by a three-dimensional non-premixed cylindrical combustion chamber. The numerical simulations are carried out using the calculation code CFD "FLUENT". Mathematical methods were used to solve the Navier-Stokes equations governing the flow phenomenon. **Findings**: The numerical results are compared and validated with the experimental data. In these conditions, the same parameters considered previously are used in the study of combustion behavior. The parameters characteristics of the flow were characterized such as the axial velocity, the temperature and the mass fraction of the carbon monoxide CO. **Application/Improvements:** The results show that the variation of the fuel influences the considered parameters. In addition, we confirm that hydrogen is a clean fuel without emitting CO into the environment.

Keywords: CFD, Hydrogen, Methane, Numerical Simulation, Premixed Combustion, Turbulence

1. Introduction

The majority of aerospace engines, such as turbojet engines and rocket engines, operate due to the combustion process, which is also responsible on the formation of pollutant chemicals that are harmful to nature[1,2]. One of the major difficulties encountered in the development of these systems is the ability to control the aerothermo chemical conditions prevailing in the combustion chamber at all engine operating ranges (taxiing, take-off or cruising). The optimization of combustion systems requires the study and analysis of the interactions of all these phenomena, which are strongly coupled[3]. This fact is done through both experimental and numerical approaches. The last approach is the most used. Indeed, the computer tool is increasingly used for engine design because of the high cost of prototypes and experimental measurement techniques and the ever-increasing speed of computers associated with the development of commercial CFD software and the constant improvement of numerical models[4,5]. On the one hand, there is the modelling and simulation of the turbulence aspect of the combustion, and on the other hand there is the modelling of the chemical kinetics of combustion[6-8]. Among the approaches dedicated to turbulence modelling are Large Eddy Simulation (LES) and the Probability Density Function (PDF) which are modern and highly sophisticated methods and which until recently were limited to the academic applications. In industrial gas burners, a jet of combustible gas is often injected into the centre of a peripheral air flow in the same direction. Again turbulence plays a beneficial role to mix the gases in the presence, combustion gas and fuel gas but also gas burn. This is due in large part to the high velocity gradient between the air

**Author for correspondence*

and gas velocity. Experience shows that the length of a turbulent diffusion flame does not depend on the rate of arrival of gas, when the stabilization is successful, whereas that of a laminar diffusion flame is proportional to this. In this way the length of the flame does not increase even for large gas flows in the burner[9].

In the present study, the objective is to study the numerical simulation of a non-premixed turbulent combustion in a cylindrical burner supplied by methane-hydrogen/air. The calculation was carried out using mathematical models in order to overcome the closure of the system of aerothermo chemical balance equations. Particularly, we have used the CFD code Fluent, to calculate the mean axial velocity, the temperature and the mass fraction of carbon monoxide CO. In the first step, we validate the mathematical models[10-13] with the experimental data in the same stations and the same conditions. The results show that the select models give a satisfactory agreement with all considered regions. In the second step, the same parameters considered previously are used in the study of the combustion behavior of methane-hydrogen fuels. The two fuels CH_4 and H_2 are compared in order to choose the least carried out on the environment. The obtained results confirm that hydrogen is considered a clean non-polluting fuel compared to methane.

2. Material and Methods

2.1 Equation of Mathematical Model

In this study, we studied the behavior of non-premixed turbulent combustion in three dimensions using calculation of the CFD code Fluent. We can write the control equations for the compressible flux in Cartesian coordinates[9-13].

The continuity equation is written in the following form:

$$\frac{\partial \overline{\rho}}{\partial t} + \frac{\partial}{\partial x_i}(\overline{\rho}\widetilde{u_i}) = 0 \quad (1)$$

The momentum equations are written:

$$\frac{\partial \overline{\rho}\widetilde{u_i}}{\partial t} + \frac{\partial}{\partial x_i}(\overline{\rho}\widetilde{u_i}\widetilde{u_j}) = -\frac{\partial}{\partial x_i}[\overline{\rho}(\overline{u_i u_j} - \widetilde{u_i}\widetilde{u_j}] - \frac{\partial \overline{p}}{\partial x_j} + \frac{\partial \overline{\tau_j}}{\partial x_i} \quad (2)$$

The energy equation is written:

$$\frac{\partial}{\partial t}\overline{\rho h} + \frac{\partial}{\partial x_i}(\overline{\rho}\widetilde{u_i}\widetilde{h}) = -\frac{\partial}{\partial x_i}[\overline{\rho}(\overline{u_i h} - \widetilde{u_i}\widetilde{h}] + \frac{\partial \overline{p}}{\partial t} + \frac{\partial}{\partial x_i}\overline{u_j \tau_j} \quad (3)$$

The species equations are written:

$$\frac{\partial}{\partial t}\overline{\rho}\widetilde{Y_f} + \frac{\partial}{\partial x_i}(\overline{\rho}u_i\widetilde{Y_f}) = -\frac{\partial}{\partial x_i}[\overline{\rho}(\overline{u_i Y_f} - \widetilde{u_i}\widetilde{Y_f}] + \overline{\dot{\omega}}_f \quad (4)$$

Where: i = 1, 2, 3 and j = 1, 2, 3, $\overline{\rho}, \widetilde{u_i}, \overline{\omega_i}$, t are density, velocity vector, fuel reaction rate and time respectively.

The Thermodynamic state is defined as follows:

$$\overline{p} = \overline{\rho} R_m \widetilde{T} \quad (5)$$

In these equations, the unresolved Reynolds stresses $(\overline{u_i u_j} - \widetilde{u_i}\widetilde{u_j})$ require a sub grid scale turbulence model. The unresolved species fluxes $(\overline{u_i Y_f} - \widetilde{u_i}\widetilde{Y_f})$ and the enthalpy fluxes $(\overline{u_i h} - \widetilde{u_i}\widetilde{h})$

Require a probability density function (PDF) approach. The filtered chemical reaction rate is characterized by $\overline{\dot{\omega}}_f$.

The tensor of the unsolved constraints τ_{ij} as the tensor velocity of deformation $\widetilde{S_{ij}}$ for sub grid models by the intermediary of a turbulent viscosity (ν_t), and a sub grid kinetic energy (k_l). Therefore, we focus on the assumption of Boussinesq in which the small scales influence the large scales via the sub grid-scale stress[9-13]:

$$\tau_{ij} = 2\overline{\rho}\nu_t \widetilde{S_j} - \frac{1}{3}k_l \delta_j \quad (6)$$

Where, the filtered strain rate tensor is defined by:

$$\widetilde{S_{ij}} = \frac{1}{2}\left(\frac{\partial \widetilde{u_i}}{\partial x_j} + \frac{\partial \widetilde{u_j}}{\partial x_i}\right) - \frac{1}{3}\widetilde{u_l}\,\delta_j \quad (7)$$

The use of this WALE-eddy viscosity model to express the eddy viscosity term in the momentum equation (2) is motivated by:

- Recovering the proper behavior of the eddy viscosity near the wall in the case of the wall-bounded flows;
- Preserving the interested properties such as the capacity to provide no eddy-viscosity in the case of vanishing turbulence (property required for the transition from laminar to turbulent states);
- Relying on the fact that no information about the direction and distance from the wall are needed (avoiding the use of any damping function);
- Being suitable for unstructured grids, where evaluating a distance to the wall is precarious.

The residual stress tensor of the WALE eddy viscosity model can be found as[3-9]:

$$\nu_t = (C_w\Delta)^2 \frac{(s_j^d s_j^d)^{3/2}}{(\widetilde{s}_j\ \widetilde{s}_j)^{5/2} + (s_j^d s_j^d)^{5/4}} \quad (8)$$

Where $s_{ij}^d = \frac{1}{2}(\widetilde{g}_j^2 + \widetilde{g}_j^2) - \frac{1}{3}\widetilde{g}_k^2\,\delta_j$ (9)

And $\widetilde{g}_{ij} = \frac{\partial \widetilde{u}_i}{\partial x_j}$ (10)

Cw: is the WALE model constant (*Cw*=0.49). The model constants used for all the computations in this paper have been set up for academic configurations such as turbulent combustion and homogenous isotropic turbulence[9-13] and, Δ is the spatial filter width.

The statistical distribution function of the mixture fraction performs much better than the commonly used sub grid scale models perform for the mixture fraction variance. Therefore, the mixture fraction is considered as the scalar variable[9-13]:

$$\tilde{y} = \int_{Z=0}^{1} y(Z)\tilde{P}(Z)dZ \quad (11)$$

With a simple global reaction rate, non-premixed combustion can be presented by a reactant mass fraction $Y_f(\vec{x},t)$, which is described in (4)[9-13].

For non-premixed combustion, additional scalar variable of mixture fraction $\widetilde{Z}(\vec{x},t)$ is needed. The transport equation of mixture fraction is such as:

$$\frac{\partial}{\partial t}\overline{\rho}\widetilde{Z} + \frac{\partial}{\partial x_i}(\overline{\rho}u_i\widetilde{Z}) = \frac{\partial}{\partial x_i}(\overline{\rho}D\frac{\partial}{\partial x_i}\widetilde{Z}) \quad (12)$$

The above two equations can be combined to be applied in whichever premixed, partially premixed, or non-premixed flames[9-13]. In the case of simple global reaction rate, progress variable $\widetilde{c}(\vec{x},t)$ is often used instead of $\widetilde{Y}_f(\vec{x},t)$ for convenience. In the thin premixed flame, progress variable changes from zero to unity. And with progress variable and mixture fraction, lean reactant mass fraction can be defined by:

$$\widetilde{Y}_f(\vec{x},t) = Y_\phi\ [\widetilde{c}(\vec{x},t),\ \widetilde{Z}(\vec{x},t)] \quad (13)$$

But for the premixed combustion with co flow of air or pilot product, following equation can be applied to express the lean reactant mass fraction[9-13],

$$\widetilde{Y}_f(\vec{x},t) = Y_\phi\ .\ \widetilde{Z}(\vec{x},t).\ [1\text{-}c(\vec{x},t)] \quad (14)$$

Y_ϕ Is the mass fraction of fuel in the main fuel/air mixture inflow?

For the unburnt reactants $\widetilde{Z}=1$ and $\widetilde{c}=0$;
For the burnt product $\widetilde{Z}=0$ and $\widetilde{c}=1$.

For homogenous combustion $\widetilde{Z}(\vec{x},t)$, the equation (14) is reduced to traditional progress variable equation for non-premixed combustion[9-14]:

$$\frac{\partial\overline{\rho}\widetilde{c}}{\partial t} + \frac{\partial}{\partial x_i}(\overline{\rho}\widetilde{u}_i\widetilde{c}) = -\frac{\partial}{\partial x_i}\tau_c + \frac{\partial}{\partial x_i}(\overline{\rho}D\frac{\partial}{\partial x_i}\widetilde{c}) + \overline{\rho\dot{\omega}_c} \quad (15)$$

In this work, the PDF method is employed as a Sub Grid Scale (SGS) closure in LES of a turbulent non-premixed combustion of methane-hydrogen/air. The joint probability density function of the SGS scalars is determined via the solution of its modeled transport equation.

2.2 Experimental Configuration and Application Domain

The configuration which confines the combustion chamber is given in Figure 1. It was a matter of numerous experimental researches because of its relatively simple geometry and its similarity to the gas turbine burner. The cylindrical combustion chamber[9-14], presenting a radius R4=61.15 mm and a length L=1 m, is provided by two coaxial jets CH_4 or H_2/air. The central jet presents an internal radius equal to R1=31.57 mm and an external radius R2=31.75 mm, in order to inject methane or hydrogen with an inlet velocity V1=92.78 cm/s at a temperature equal to T1=300 K. The annular jet has an internal radius equal to R3=46.85 mm, which injects air with an inlet velocity equal to V2=20.63 m/s and a preheated temperature T2=750 K. The chamber of Combustion is pressurized by a value equal to p=3.8 atm and a constant temperature wall equal to T=500 K. The presentation and comparison of the results are based on the normalization of length and velocity using the radius of the injector (R≡R3) and the velocity of the inlet air (U≡V2).The equations of the balance sheet are solved by the finite volume method. In our case, the grid used for all the simulation is realized by Gambit. In these conditions, the meshes used are of the parallelepiped type. The grid is smooth and refined for the nearly solid limits of the burner and in the longitudinal direction in the interaction level of air and fuel, to receive more information in the solid boundary and the flame zone. The volume contains about 2.7 million cells. The size of a cell ranges between 3.057304 10^{-9} m^3 and 2.934596 10^{-7} m^3.

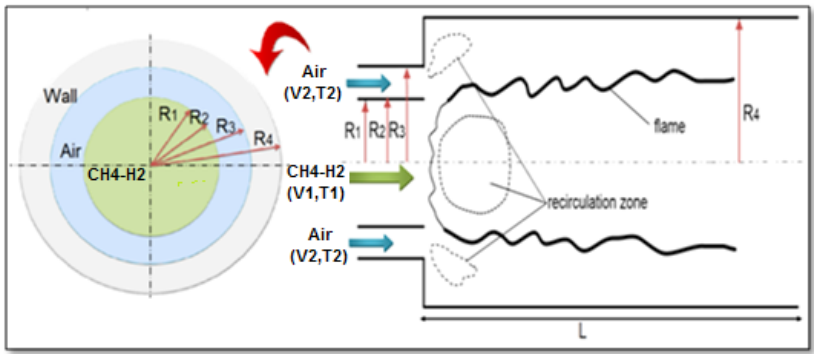

Figure 1. Geometric Parameters of the Combustion Chamber.

3. Result and Discussion

In this study, a comparison of our results and those obtained experimentally for the profiles of the axial velocity, temperature and mass fraction of carbon monoxide 'CO', shows a good agreement of the results. In addition, the same parameters used for validation are also used to control the flame behaviour provided by CH_4 or H_2.

3.1 Models Validation

3.1.1 Axial Velocity

Figure 2 illustrates the comparison of the radial profiles of the mean axial velocity between the numerical calculations and the experimental data[14]. These results are presented in the x/R=0.38 and x/R=1.27 stations. Globally, numerical and experimental results have almost the same tendency. Thus, the high values of the axial velocity are located in the center of the chamber presented by the peaks in the stations previously. The creation of the recirculation zones upstream from the wall is due to the sudden widening of the combustion chamber generating a sudden variation in the parameters (surface, pressure, etc.), which can be explained by the significant negative values observed close to the wall presented in the two stations x/R=0.38 and x/R=1.27. A second recirculation zone, caused by the delayed flow, occurred at the centre of the combustion chamber. The delayed flow of methane produces shears which give rise to this recirculation zone. The zone of the flame is the seat of the great values of the speed. The results obtained from the simulation carried out in this study show that the velocity field is sensitive to heat, chemistry and geometry. The mean relative gap between the numerical calculations and the experimental reference data[14] is about 7%. These results confirm the validation of the numerical method.

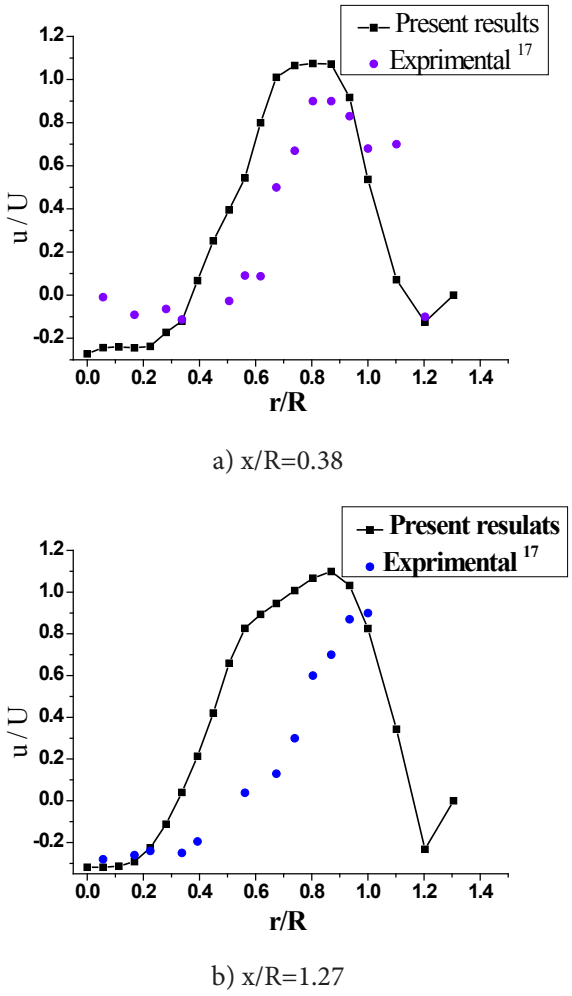

a) x/R=0.38

b) x/R=1.27

Figure 2. Radial Profiles of the Axial Velocity.

3.1.2 Temperature

As presented in Figure 3, the obtained temperature profiles are in good agreement with those of the experiment considered in reference[14], for the stations defined by x/R=0.89 and x/R=5.20. Numerical and experimental profiles have almost the same tendency. The high temperature values are located in the flame area and the temperature begins to decrease with the increase of the radial distance. The observed difference between the numerical and experimental results can be explained by the experimental conditions where the walls are cooled by water to keep a constant temperature equal to T=500 K[10-14], which cannot achieve the wall condition isotherm. However, in our simulation calculations, the walls are considered isothermal. On the other hand, the deviations obtained can be justified by the uncertainties of the instrumentation of temperature measurement (thermocouple). The average of relative gap between the numerical calculations and the experimental reference data is about 10%.

3.1.3 CO Mass Fraction

The flame region is rich in carbon monoxide 'CO' which is a resultant species of combustion. Figure 4 illustrates the simulation results in good agreement with experimental[14] of the mass fraction of carbon monoxide CO for different stations defined by x/R=3.16 and x/R=7.41. The results obtained show that the temperature behaves in the same way as the mass fraction of the carbon monoxide CO. The temperature is high in the area of the flame and decreases as the flame moves away. This is the same trend observed for the evolution of the mass fraction of CO. Chemical reactions and soot formation generates radiation accumulation, which causes an increase in temperature in the different areas of the flame. The gap between the numerical results and the experimental data is about 5%.

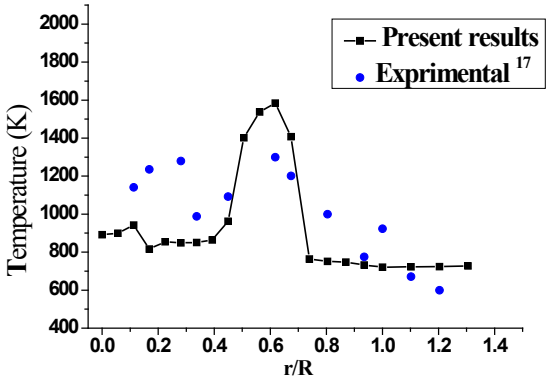

a) x/R=0.89

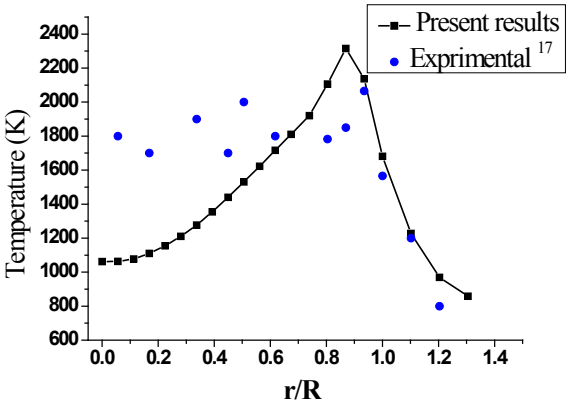

b) x/R=5.20

Figure 3. Radial Profiles of Mean Temperature.

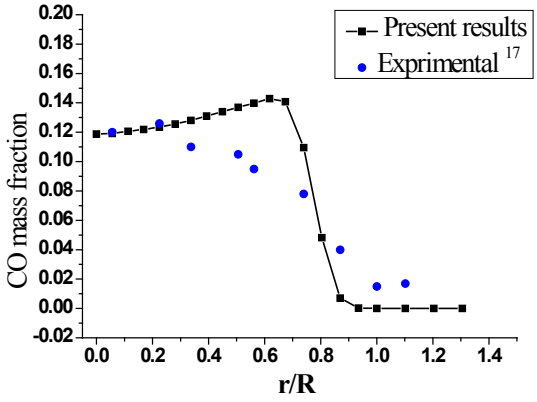

a) x/R=3.16

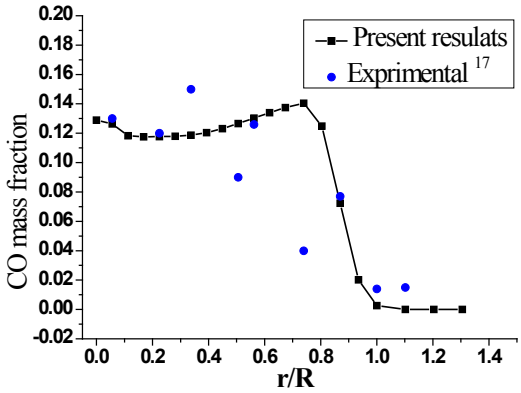

b) x/R=7.41

Figure 4. Radial Profiles of CO Mass Fraction.

3.2 The Behavior of these Parameters due to the Variation of CH_4-H_2 Fuels

3.2.1 Axial Velocity

Figure 5 illustrates the comparison between the radial profiles of the mean axial velocity of H_2 and CH_4. These profiles are characterized by the peaks in the different stations defined by x/R=0.38 and x/R=1.27. The numerical profiles of the H_2 have the same shape with the profiles of CH_4. The curves present a variation of the average speed in the cylindrical combustion chamber not premixed over the radial distance. Indeed, it has been noted that the different profiles are superimposed in the same way as a slight increase in the average speed which is affected by the fuel H_2 and the values of hydrogen velocity elevated with respect to the values of the methane in the two stations. The velocity values of the hydrogen are higher than in the second station. Thus, we can also see negative values in the velocity profiles in the x/R=0.38 and x/R=1.27 which correspond to the recirculation regions in the centre of the burner and close to the walls. In these conditions, the values of the axial velocity in the middle of the combustion chamber are higher with H_2 compared with CH_4, especially in the first station. Thus, we can also see the profiles of the H_2 speed completely applicable on the CH_4 profiles near the burner walls in both stations. Indeed, it has been observed that the axial velocity of hydrogen is greater than the rate of methane almost the mass of hydrogen is less than the mass of methane.

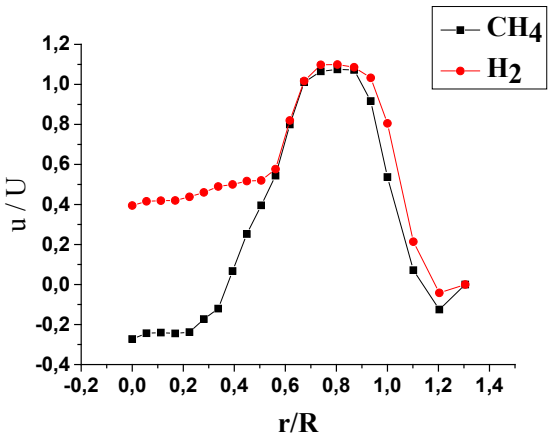

a) x/R=0.38

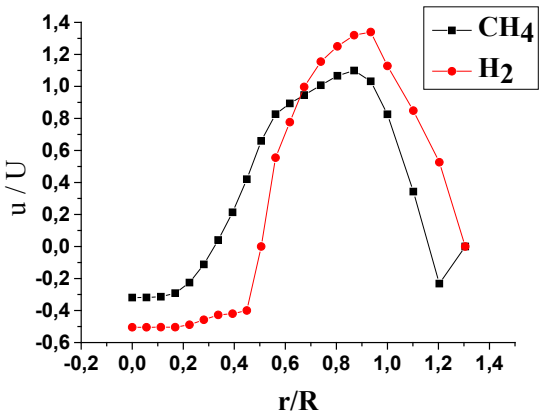

b) x/R=1.27

Figure 5. Profiles of the Axial Velocity Considered for H_2 and CH_4.

3.2.2 Temperature

The distribution of the average temperature of hydrogen and methane in a non-premixed combustion chamber is shown in Figure 6. In the flame area, the radial temperature profiles show peaks in the stations defined by x/R=0.89 and x/R=5.20 and then decrease to the wall temperature equal to T=500 K. The high temperature values are located in the flame area for the two fuels H_2 and CH_4. The same chemical reaction zone and these reactions are considered as exothermic reactions. The temperature values decrease as we move away from the flame zone, with a slight increase in H_2 temperature values relative to CH_4. Moreover, it should be noted that the temperature in the two curves takes the same shape with different values, and the positions of the peaks displace at the jet of air for the case of H_2. In the case of CH_4 fuel, it has been noted that the extreme of the curve corresponds to a temperature equal to T=900 K in the middle of the combustion chamber at T=600 K for the H_2 fuel in the first case defined by x/R=0.89. On the other hand, in the second case defined by x/R=5.20, the extreme of the curve in the centre of the burner for CH_4 of temperature variation corresponds to an equal value at T=1100 K and at T=600 K for the hydrogen.

3.2.3 CO Mass Fraction

In this section, we choose carbon monoxide as a chemical species of pollutant. The carbon monoxide field is varied between two stations x/R=3.16 and x/R=7.41 in Figure 7. The comparison is made between the mass fraction of the carbon monoxide 'CO' produced during the combustion

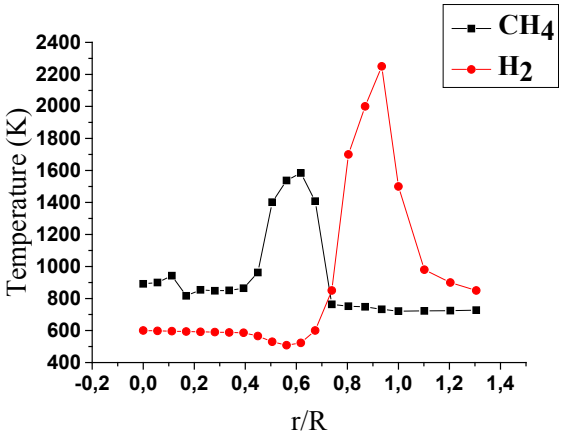

a) x/R=0.89

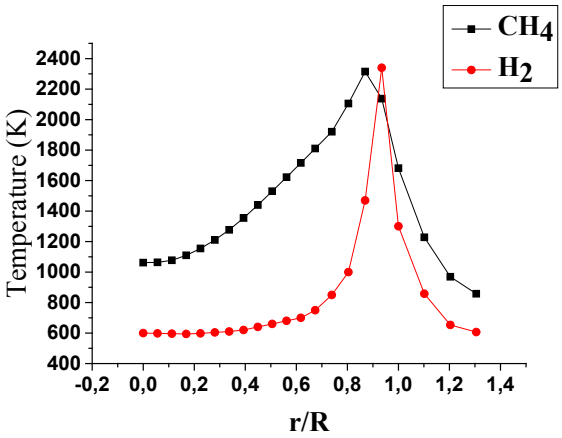

b) x/R=5.20

Figure 6. Profiles of the Temperatures Considered for H_2 and CH_4.

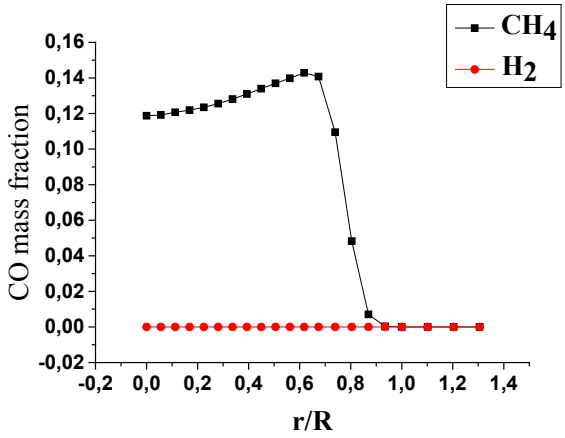

a) x/R=3.16

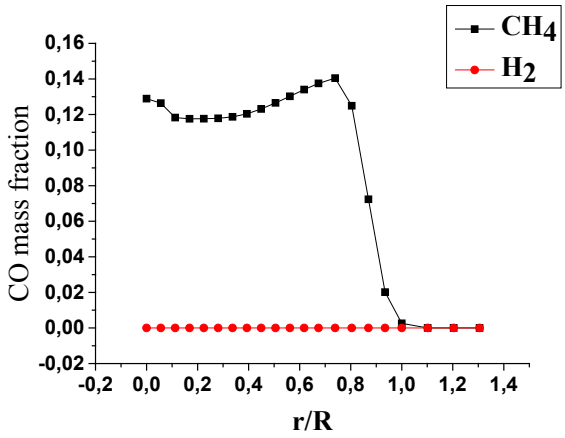

b) x/R=7.41

Figure 7. Radial Profiles of CO Mass Fraction Considered for H_2 and CH_4.

of the fuel H_2 and CH_4 with the air. The results clearly illustrate that the values of the fuel CO of hydrogen is a much lower amount compared to the fuel of methane. The obtained results show that the temperature behaves in the same way as the mass fraction of the carbon monoxide CO. This means that the region of the flame is rich in CO which is a species produced by combustion. In the first case defined by x/R=3.16, it has been noted that the extremity of the methane curve corresponds to a mass fraction of CO equal to yco=0.13 which is located in the r/R=0.7 position. In the second case defined by x/R=7.41, the extremity of the CH_4 curve corresponds to a CO mass fraction equal to yco=0.14 which is located in the r/R=0.6 position, where the mass fraction of CO of the hydrogen curve is equal to yco=0 over the entire radial distance. However, the CO produced by the combustion of H_2 is equal to 0 in all the stations of the combustion chamber.

4. Conclusion

In this study, we have developed numerical calculations using the CFD-FLUENT tools in a simple 3-D geometry fed by two methane-hydrogen/air fuels. Moreover, we have studied the behavior of combustion of fuels CH_4-H_2. The obtained results confirm that:

- The simulation results of this work are in good agreement with those of the experiment.
- The emission of carbon monoxide is non-existent for combustion of hydrogen in the combustion chamber at all stations, but exists for methane.

- Higher temperature for hydrogen fuel was observed compared to methane fuel in different stations.
- The results show that the hydrogen velocity field is faster than that of methane since the molar mass of hydrogen is smaller than methane.
- After comparing the CH_4 and H_2 fuels to choose the least carried out on the environment, the results obtained that hydrogen is a clean non-polluting fuel compared to methane.

With these results, we confirm that hydrogen fuel is better than methane, which is cleaner and less harmful to the environment.

This study can be extended to include the effects of instabilities and to use the pollutant model to determine the fractions species of the OH radicals and emissions of NOx.

5. References

1. Bourghi R, Destiau M, DE Soete G. La combustion et les flammes. Technip-Paris. 1996; 42(10):1993-2994.
2. Bourghi R, Champion M. Modelisation et theorie des flammes. Technip- Paris. 2000 February; p. 1-384.
3. Pierce CD. University of Stanford, USA: Progress-variable approach for large-eddy simulation of turbulent combustion, Ph.D. Thesis. 2001; 62-09:1-4189.
4. Shah RR, Kulshreshtha DB. Analytical and Numerical Analysis of Micro Combustor for Gas Turbine Engine. Indian Journal of Science and Technology. 2016; 9(48):1-6.
5. Domingo P, Vervisch L, Payet S, Hauguel R. DNS of a premixed turbulent V flame and LES of a ducted flame using a FSD-PDF subgrid scale closure with FPI-tabulated chemistry. Combustion and Flame. 2005; 143(4):566-86. Crossref.
6. Pitsch H, Fedotov S. Investigation of scalar dissipation rate fluctuations in nonpremixed turbulent combustion using a stochastic approach. Combust Theory Modeling. 2001; 5(1):41-57. Crossref.
7. Goldin GM, Menon S. A Scalar PDF Construction Model for Turbulent Non-Premixed Combustion. Combustion Science and Technology. 1997; 125(1-6):47-72. Crossref.
8. Klimenko AY. Matching conditional moments in PDF modelling of non-premixed combustion. Combustion and Flame. 2005; 143(4):369-85. Crossref.
9. Attia MEH, Driss Z, Khechekhouche A. Numerical Study of the Combustion of CH4-C3H8/ Air: Application to a Combustion Chamber with Two Coaxial Jets. International Journal of Energetica (IJECA). 2017; 2(2):38-42.
10. Bouras F, Attia MEH, Khaldi F, SI-AMEUR M. Control of the Methane Flame Behavior by the Hydrogen Fuel Addition: Application to Power Plant Combustion Chamber. International journal of Hydrogen energy. 2017; 42:8932-39. Crossref.
11. Bouras F, Attia MEH, Khaldi F. Optimisation of Entropy Generation in Internal Combustion Engine. Environmental Process. 2015; 2:233-42. Crossref.
12. Bouras F, Attia MEH, Khaldi F, SI-AMEUR M. Control of the Methane Flame Behavior by the Hydrogen Fuel Addition: Application to Power Plant Combustion Chamber. Proceedings of Engineering & Technology (PET). IPCO-2016. 2016; 13:114-18.
13. Bouras F, Attia MEH, Khaldi F. Improvements of the Combustion Characteristics by the Hydrogen Enrichment. IEEE Xplore. 2015; p. 1-5. Crossref.
14. Pierce CD, Moin P. Progress-variable approach for large-eddy simulation of non-premixed turbulent combustion. Journal of Fluid Mechanics. 2004 April; 504:73-97. Crossref.